5814 *Chem. Mater.* **2010,** *22,* 5814–5822
DOI:10.1021/cm101407d

CHEMISTRY OF
MATERIALS
Article

Ion Conduction in Imidazolium Acrylate Ionic Liquids and their Polymers

Minjae Lee,[†] U Hyeok Choi,[‡] Ralph H. Colby,*[,‡] and Harry W. Gibson*[,†]

[†]*Department of Chemistry, Virginia Polytechnic Institute and State University, Blacksburg, Virginia 24061, United States, and* [‡]*Department of Materials Science & Engineering, Pennsylvania State University, University Park, Pennsylvania 16802, United States*

Received May 18, 2010. Revised Manuscript Received September 21, 2010

Polymerizable imidazolium acrylates and their polymers with pendant imidazolium cations were synthesized with hexafluorophosphate and bis(trifluoromethanesulfonyl)imide counterions and characterized using calorimetry and dielectric spectroscopy. The ionic polymers containing a diethyleneoxy unit as an N-substituent on the imidazolium cation display higher ionic conductivities than the analogous N-*n*-butyl polymers. Using a physical model of electrode polarization, we separate the conductivity of single-ion conductors into number density of conducting ions p and their mobility μ. The monomers invariably possess higher conducting ion number density than the polymers, owing to the cation being part of the polymer, but p is insensitive to the N-substituent. In contrast, the diethyleneoxy N-substituent imparts higher mobility than the *n*-butyl N-substituent, for both monomers and polymers, owing to a lower binding energy between the imidazolium and the counteranions, which is *not* directly reflected in glass transition temperatures.

Introduction

For the last few decades, the impact of ionic liquids (ILs) on chemical and material sciences has evolved from "green chemicals" in organic reactions to functional integration into electromechanical devices and high-performance membranes.[1] ILs have been studied widely because of their unique characteristics, such as low-volatility, nonflammability, large electrochemical window, and high ionic conductivity.[2−11]

Polymerizable ionic liquid monomers and their polymers have been studied for use as high-performance single-ion-conducting membranes. Polymerizations of 1-alkyl-3-vinylimidazolium salts and their conducting properties were studied by Ohno and co-workers.[12] They also changed the pendant structures of polymers by introduction of polymerizable (meth)acrylate moieties; imidazolium units placed at the end of longer brush pendant chains afforded higher conductivities than shorter brush polymers.[13,14] Polystyrenes with phenylimidazolium groups were also studied by Ohno et al. In some cases, the polymer−lithium salt composites showed higher conductivities than the polymers by themselves, and the ionic conductivity increased upon addition of up to 1 equivalent of lithium salt per ionic unit.[15] A new class of ionic liquid monomers, formed by neutralization of long chain acids and *N*-monoalkylimidazoles, was also prepared and their polymerizations were studied.[16,17] Solution properties of polymerized ionic liquid monomers and electrospun fibers from the polymers were observed by Elabd et al.[18] They also studied the effect of random copolymer compositions from imidazolium methacrylate and hexyl acrylate on ion conduction.[19] The properties of liquid crystalline imidazolium polymers have also been reported.[20−23] Anisotropic conductivities were observed from homeotropic one-dimensional alignment and photopolymerization of ionic liquid crystals on modified glass surfaces.[23]

Herein, we report new polymerizable acrylate monomers with imidazolium units. We polymerized those

---

*To whom correspondence should be addressed. E-mail: rhc5@psu.edu, hwgibson@vt.edu.

(1) Davis, J. H., Jr.; Fox, P. A. *Chem. Commun.* **2003**, 1209.
(2) Wilkes, J. S.; Zaworotko, M. J. *J. Chem. Soc., Chem. Commun.* **1992**, 965.
(3) Welton, T. *Chem. Rev.* **1999**, *99*, 2071.
(4) Xu, W.; Cooper, E. I.; Angell, C. A. *J. Phys. Chem. B* **2003**, *107*, 6170.
(5) Miao, W.; Chan, T. H. *Acc. Chem. Res.* **2006**, *39*, 897.
(6) Lee, S.-G. *Chem. Commun.* **2006**, 1049.
(7) El Seoud, O. A.; Koschella, A.; Fidale, L. C.; Dorn, S.; Heinze, T. *Biomacromolecules* **2007**, *8*, 2629.
(8) Headley, A. D.; Ni, B. *Aldrichimica Acta* **2007**, *40*, 107.
(9) Forsyth, S. A.; Fröhlich, U.; Goodrich, P.; Gunaratne, H. Q. N.; Hardacre, C.; McKeown, A.; Seddon, K. R. *New J. Chem.* **2010**, *34*, 723.
(10) Bara, J. E.; Camper, D. E.; Gin, D. L.; Noble, R. D. *Acc. Chem. Res.* **2010**, *43*, 152.
(11) Green, M. D.; Long, T. E. *Polym. Rev.* **2009**, *49*, 291.
(12) Ohno, H.; Ito, K. *Chem. Lett.* **1998**, 751.
(13) Yoshizawa, M.; Ohno, H. *Electrochim. Acta* **2001**, *46*, 1723.
(14) Ohno, H. *Electrochim. Acta* **2001**, *46*, 1407.
(15) Hirao, M.; Ito-Akita, K.; Ohno, H. *Polym. Adv. Technol.* **2000**, *11*, 534.
(16) Ohno, H.; Yoshizawa, M.; Ogihara, W. *Electrochim. Acta* **2004**, *50*, 255.
(17) Juger, J.; Meyer, F.; Vidal, F.; Chevrot, C.; Teyssie, D. *Tetrahedron Lett.* **2009**, *50*, 128.
(18) Chen, H.; Elabd, Y. A. *Macromolecules* **2009**, *42*, 3368.
(19) Chen, H.; Choi, J.-H.; Salas-de la Cruz, D.; Winey, K. I.; Elabd, Y. A. *Macromolecules* **2009**, *42*, 4809.
(20) Takada, S.; Suzuki, N.; Mihara, T.; Koide, N. *Mol. Cryst. Liq. Cryst.* **2004**, *419*, 87.
(21) Yoshizawa, H.; Mihara, T.; Koide, N. *Liq. Cryst.* **2005**, *32*, 143.
(22) Binnemans, K. *Chem. Rev.* **2005**, *105*, 4148.
(23) Yoshio, M.; Kagata, T.; Hoshino, K.; Mukai, T.; Ohno, H.; Kato, T. *J. Am. Chem. Soc.* **2006**, *128*, 5570.

monomers using free radical methods and studied both monomers and polymers using DSC to measure the glass transition temperatures T_g. Using dielectric spectroscopy we assessed ionic conductivities and dielectric constants of these monomers and polymers; we also analyzed the macroscopic electrode polarization at lower frequencies in dielectric measurements to determine the number density of conducting ions and their mobility,[24−27] a method which has recently been utilized with great success for single-ion conductors above T_g.[28−30]

Experimental Procedures

Instruments. ^{1}H and ^{13}C NMR spectra were obtained on Varian Inova 400 MHz and Unity 400 MHz spectrometers. High-resolution electrospray ionization time-of-flight mass spectrometry (HR ESI TOF MS) was carried out on an Agilent 6220 Accurate Mass TOF LC/MS Spectrometer in positive ion mode. Differential scanning calorimetry (DSC) with heating and cooling rates of 5 or 10 K/min on $\sim$10-mg samples was done using a TA Instrument Q2000 differential scanning calorimeter. The thermal stabilities of these polymers were studied under N_2 using a TA Instrument Q500 Thermogravimetric Analyzer at a heating rate of 10 K/min heating under N_2 purge.

Size Exclusion Chromatography. The molecular weight estimation on polymer **4d** was made on a Waters Breeze 2 system at 40 °C using Styragel@HR 3 and Styragel@HR 4 columns, covering the range from 500 to 600,000 Da, a refractive index detector, a solution of polymer in 0.05 M LiBr in DMF (2 mg/mL), and a flow rate of 1.0 mL/min. The molecular weights are referenced to poly(ethylene glycol)/poly(ethylene oxide) (PEG/PEO) standards (Fluka Analytical).

Dielectric Spectroscopy. The ionic conductivity measurements of the monomers and polymers were performed by dielectric spectroscopy using a Novocontrol GmbH Concept 40, with 0.1 V amplitude and 10^{-2} to 10^7 Hz frequency range. Samples were prepared for the dielectric measurements by allowing them to flow to cover a 30-mm diameter polished brass electrode at 100 °C *in vacuo* to form a puddle deeper than 50 μm with several 50-μm silica spacers immersed. Then a 15-mm diameter polished brass electrode was placed on top to make a parallel plate capacitor cell which was squeezed to a gap of 50 μm in the instrument (with precise thickness checked after dielectric measurements were complete). Each sample was annealed in the Novocontrol at 120 °C in a heated stream of N_2 for 1 h prior to measurements. Data were collected in isothermal frequency sweeps from 120 °C to near T_g.

Materials. 2,2′-Azobisisobutyronitrile (AIBN) was recrystallized from chloroform below 40 °C and dried in a vacuum oven and stored in a freezer ($\leq$10 °C). Acetonitrile (MeCN) for polymerizations was distilled over calcium hydride. All other chemicals and solvents were used as received.

1-[2′-(2″-Methoxyethoxy)ethyl]imidazole (***1***). A mixture of imidazole (2.04 g, 30 mmol), NaOH 50% solution (2.88 g, 30 mmol) in THF (35 mL) and 2-(2′-methoxyethoxy)ethyl *p*-toluenesulfonate (8.23 g, 30 mmol) was refluxed for 2 days. After cooling and removal of all solvents under vacuum, the mixture was extracted 3 times with CH_2Cl_2/H_2O. The combined organic layer was washed with water and dried over anhydrous Na_2SO_4. The drying agent was removed by filtration and the solvent was removed in a rotoevaporator. A yellow liquid (5.22 g, 100%) was obtained after drying in a N_2 stream. ^{1}H NMR (400 MHz, $CDCl_3$, 23 °C): δ 3.37 (s, 3H), 3.51 (m, 2H), 3.57 (m, 2H), 3.74 (t, J = 5, 2H), 4.12 (t, J = 5, 2H), 6.99 (s, 1H), 7.04 (s, 1H), 7.53 (s, 1H). ^{13}C NMR (100 MHz, $CDCl_3$, 23 °C): δ 46.9, 59.0, 70.5, 70.6, 71.7, 119.3, 129.1, 137.4. The ^{1}H NMR spectral data are exactly the same as reported in the literature.[31]

1-[2′-(2″-Methoxyethoxy)ethyl]-3-(ω-carboxypentyl)imidazolium PF_6^- (***2a***). A solution of **1** (2.553 g, 15 mmol) and 6-bromohexanoic acid (2.926 g, 15 mmol) in THF (15 mL) was refluxed for 3 days. After the reaction mixture was cooled to room temperature, the THF was decanted off and the residue was washed with THF and ethyl ether 3 times each. The bromide salt was dissolved in water (15 mL), and KPF_6 (3.04 g, 17 mmol) was added. The mixture was stirred for 1 h at room temperature. The precipitated oily product was washed with ethyl ether 5 times. Drying in a vacuum oven gave a yellow viscous liquid: 3.10 g (48%). ^{1}H NMR (400 MHz, acetone-d_6, 23 °C): δ 1.42 (m, 2H), 1.64 (m, 2H), 2.00 (m, 2H), 2.31 (m, 2H), 3.30 (s, 3H), 3.49 (m, 2H), 3.65 (m, 2H), 3.92 (t, J = 5, 2H), 4.40 (t, J = 7, 2H), 4.53 (t, J = 5, 2H), 7.78 (m, 2H), 9.07 (s, 1H). ^{13}C NMR (100 MHz, acetone-d_6, 23 °C): δ 25.4, 26.6, 29.5, 29.8, 29.95, 30.02, 30.1, 30.5, 34.5, 50.7, 50.9, 69.5, 70.6, 72.1, 123.4, 124.7, 136.7, 176.2. HR MS: m/z 285.1801 ($[M - PF_6]^+$, calcd. for $C_{14}H_{25}N_2O_4$ 285.1814, error 4.6 ppm).

1-Butyl-3-(5′-carboxypentyl)imidazolium PF_6^- (***2b***). A mixture of *N*-butylimidazole (5.92 g, 47.7 mmol) and 6-bromohexanoic acid (9.30 g, 47.7 mmol) in THF (40 mL) was refluxed for 3 days. After the reaction mixture was cooled to room temperature, the THF was decanted off and the residue was washed with THF 3 times. The residual yellow viscous oil was dissolved in deionized water (80 mL) and then KPF_6 (10.12 g, 55 mmol) was added. The mixture was stirred for 24 h at room temperature. After decanting off the upper aqueous layer, the residual oily product was washed with deionized water 3 times. Drying in a vacuum oven gave a pale-yellow viscous liquid (11.57 g, 63%). DSC (N_2, −80 to 200 °C, heating and cooling rate 5 °C): $T_g = -39.3$ °C (2nd cycle), no other transition found. ^{1}H NMR (400 MHz, acetone-d_6, 23 °C): δ 0.95 (t, J = 8, 3H), 1.40 (m, 4H), 1.65 (m, 4H), 1.97 (m, 4H), 2.32 (t, J = 8, 2H), 4.36 (q, J = 8, 1H), 7.77 (m, 2H), 9.03 (s, 1H). ^{13}C NMR (100 MHz, acetone-d_6, 23 °C): δ 13.6, 20.0, 24.7, 26.1, 30.3, 30.6, 32.6, 33.8, 50.3, 123.5, 136.7, 174.7. HR ESI MS: m/z 239.1746 ($[M - PF_6]^+$, calcd. for $C_{13}H_{23}N_2O_2$ 239.1754, error 3.3 ppm).

1-[2′-(2″-Methoxyethoxy)ethyl]-3-(10‴-carboxydecyl)imidazolium Tf_2N^- (***2c***). A mixture of **1** (5.11 g, 31 mmol) and 11-bromoundecanoic acid (8.22 g, 31 mmol) in MeCN (60 mL) was refluxed for 4 days. After the MeCN was removed under vacuum, ethyl ether (120 mL) was added with stirring. The precipitated bromide salt was filtered and then washed with ethyl ether 3 times. The filtered solid was dissolved in deionized water (300 mL), and $LiTf_2N$ (10 g, 35 mmol) was added. The mixture was stirred for 24 h at 50 °C. After decanting off the upper aqueous layer, the precipitated oil was washed with deionized water 3 times. Drying in a vacuum oven gave a yellow−brown viscous liquid

---

[24] Macdonald, J. R. *Phys. Rev.* **1953**, *92*, 4.

[25] Coelho, R. *Rev. Phys. Appl.* **1983**, *18*, 137.

[26] Coelho, R. *Physics of Dielectrics for the Engineer*; Elsevier: New York, 1979.

[27] Barsoukov, E.; Macdonald, J. R., Eds. *Impedance Spectroscopy Theory, Experiment and Applications*; Wiley: Hoboken, 2005.

[28] Klein, R. J.; Zhang, S.; Dou, S.; Jones, B. H.; Colby, R. H.; Runt, J. *J. Chem. Phys.* **2006**, *124*, 144903.

[29] Fragiadakis, D.; Dou, S.; Colby, R. H.; Runt, J. *Macromolecules* **2008**, *41*, 5723.

[30] Fragiadakis, D.; Dou, S.; Colby, R. H.; Runt, J. *J. Chem. Phys.* **2009**, *130*, 064907.

[31] Bara, J. E.; Gabriel, C. J.; Lessmann, S.; Carlisle, T. K.; Finotello, A.; Gin, D. L.; Noble, R. D. *Ind. Eng. Chem. Res.* **2007**, *46*, 5380.

(18.22 g, 93%). DSC (N_2, −80 to 200 °C, heating and cooling rate 5 °C): T_g = −63 °C, no other transition found. ^{1}H NMR (400 MHz, CD_3CN 23 °C): δ 1.28(m, 12H), 1.55 (m, 2H), 1.82 (m, 4H), 2.26 (t, J = 7, 2H), 3.29 (s, 3H), 3.46 (t, J = 5, 2H), 3.58 (t, J = 5, 2H), 3.78 (t, J = 5, 2H), 4.12 (t, J = 7, 2H), 4.27 (t, J = 5, 2H), 7.38 (s, 1H), 7.42 (s, 1H), 8.52 (s, 1H). ^{13}C NMR (100 MHz, CD_3CN, 23 °C): δ 25.6, 26.6, 29.5, 29.7, 29.91, 29.95, 29.97, 30.5, 34.2, 50.5, 50.6, 69.1, 70.8, 72.4, 123.0, 124.0, 136.8, 175.6. HR MS: m/z 355.2606 ([M − Tf_2N^-]$^+$, calcd. for $C_{19}H_{35}N_2O_4$ 355.2597, error 2.7 ppm).

*1-Butyl-3-(10′-carboxydecyl)imidazolium Tf_2N^- (**2d**)*. A mixture of *N*-butylimidazole (6.21 g, 50 mmol) and 11-bromoundecanoic acid (13.97 g, 50.0 mmol) in THF (120 mL) was refluxed for 4 days. After the reaction mixture was cooled to room temperature, the precipitated bromide salt was filtered and then washed with cold THF 3 times. The filtered solid was dissolved in deionized water (100 mL) and $LiTf_2N$ (15.6 g, 55 mmol) was added. The mixture was stirred for 24 h at 50 °C. After decanting off the upper aqueous layer, the precipitated oil was washed with deionized water and ethyl ether 3 times each. Drying in a vacuum oven gave a yellow viscous liquid (19.4 g, 66%). DSC (N_2, −80 to 200 °C, heating and cooling rate 5 °C): T_g = −55 °C, no other transition found. ^{1}H NMR (400 MHz, acetone-d_6, 23 °C): δ 0.95 (t, J = 7, 3H), 1.30−1.40 (m, 14H), 1.58 (m, 2H), 1.97 (m, 4H), 2.27 (t, J = 7, 2H), 4.38 (t, J = 7, 2H), 7.81 (s, 2H), 9.14 (s, 1H). ^{13}C NMR (100 MHz, acetone-d_6, 23 °C): δ 13.7, 20.0, 25.7, 26.7, 29.6, 30.0, 30.7, 32.7, 34.3, 50.3, 50.6, 123.6, 136.7, 174.9. HR MS: m/z 309.2527 ([M-Tf_2N^-]$^+$, calcd. for $C_{18}H_{33}N_2O_2$ 309.2537, error 3.2 ppm).

*1-{ω-[1‴-(4‴-Acryloyloxy)butoxy]carbonylpentyl}-3-[2′-(2″-methoxyethoxy)ethyl]imidazolium PF_6^- (**3a**)*. A solution of **2a** (2.04 g, 4.75 mmol) in freshly distilled $SOCl_2$ (5 mL) was stirred for 24 h at room temperature under N_2 atmosphere. After removing the excess $SOCl_2$ under vacuum, the residue was washed with anhydrous ethyl ether 5 times and then dried by N_2 stream. The residue was dissolved in dry MeCN (5 mL), and 4-hydroxybutyl acrylate (0.822 g, 5.70 mmol) was added. Into the reaction mixture in an ice bath, triethylamine (0.484 g, 4.76 mmol) was slowly added. The reaction mixture was stirred for 24 h at room temperature. After water (10 mL) was added, the product was extracted 3 times with ethyl acetate (EA) and then the combined organic layer was dried over anhydrous Na_2SO_4. The drying agent was removed by filtration and the solvent was removed in a rotoevaporator. The product was rinsed with ethyl ether 5 times with vigorous stirring and then dried in a N_2 stream. A yellow viscous liquid (2.02 g, 76.4%) was obtained after drying. DSC (−80−60 °C, heating and cooling rate 10 °C/min., N_2): T_g = −49 °C, no other transition found. ^{1}H NMR (400 MHz, acetone-d_6, 23 °C): δ 1.42 (m, 2H), 1.61−1.76 (m, 6H), 2.00 (m, 2H), 2.33 (m, 2H), 3.30 (s, 3H), 3.49 (m, 2H), 3.65 (m, 2H), 3.93 (t, J = 5, 2H), 4.10 (m, 2H), 4.17 (m, 2H), 4.41 (t, J = 7, 2H), 4.54 (t, J = 5, 2H), 5.89 (dd, J = 10 (*cis*), J = 2 (gem.), 1H), 6.15 (dd, J = 17 (*trans*), J = 10 (*cis*), 1H), 6.35 (dd, J = 17 (*trans*), J = 2 (gem.), 1H), 7.82 (m, 2H), 9.12 (s, 1H). ^{13}C NMR (100 MHz, acetone-d_6, 23 °C): 24.8, 26.0, 26.1, 26.2, 30.4, 34.2, 50.3, 50.5, 58.8, 64.3, 64.6, 69.3, 70.8, 72.4. HR ESI MS: m/z 411.2534 ([M − PF_6]$^+$, calcd. for $C_{21}H_{35}N_2O_6$ 411.2495, error 9.4 ppm).

*1-{ω-[1′-(4′-Acryloyloxy)butoxy]carbonylpentyl}-3-butylimidazolium PF_6^- (**3b**)*. A solution of **2b** (1.78 g, 4.6 mmol) in freshly distilled $SOCl_2$ (5 mL) was stirred for 24 h at room temperature under N_2. After removal of the excess $SOCl_2$ under vacuum, the residue was washed with anhydrous ethyl ether 5 times and then dried by a N_2 stream. The residue was dissolved in dry MeCN (5 mL), and then 4-hydroxybutyl acrylate (0.801 g, 5.6 mmol) was added. Into the reaction mixture in an ice bath, triethylamine (0.468 g, 4.6 mmol) was slowly added. The reaction mixture was stirred for 24 h at room temperature. After water (20 mL) was added, the mixture was extracted 3 times with EA and then the combined organic layer was dried over anhydrous Na_2SO_4. The drying agent was removed by filtration and the solvent was removed in a rotoevaporator. The product was rinsed with ethyl ether 5 times with vigorous stirring. Drying in a vacuum oven at room temperature gave a brown viscous liquid (2.13 g, 90%). DSC (−80 to −60 °C, heating and cooling rate 5 °C/min., N_2): T_g = −58 °C, no other transition found. ^{1}H NMR (400 MHz, acetone-d_6, 23 °C): δ 0.95 (t, J = 7, 3H), 1.40 (m, 4H), 1.63−1.74 (m, 6H), 1.92−2.05 (m, 4H,), 2.33 (t, J = 7, 2H), 4.08−4.19 (m, 4H), 4.38 (m, 4H), 5.89 (dd, J = 10 (*cis*), J = 2 (gem.), 1H), 6.16 (dd, J = 17 (*trans*), J = 10 (*cis*), 1H), 6.35 (dd, J = 17 (*trans*), J = 2 (gem.), 1H), 7.80 (s, 2H), 9.09 (s, 1H). ^{13}C NMR (100 MHz, acetone-d_6, 23 °C): δ 13.7, 20.0, 24.8, 26.0, 26.1, 26.2, 30.3, 32.7, 34.1, 50.33, 50.34, 64.3, 64.6, 123.6, 129.5, 131.1, 136.8, 166.4, 173.5. HR ESI MS: m/z 365.2428 ([M − PF_6]$^+$, calcd. for $C_{20}H_{35}N_2O_4$ 365.2435, error 1.9 ppm).

*1-{ω-[1‴-(4‴-Acryloyloxy)butoxy]carbonyldecyl}-3-[2′-(2″-methoxyethoxy)ethyl]imidazolium Tf_2N^- (**3c**)*. A solution of **2c** (6.92 g, 10.9 mmol) in freshly distilled $SOCl_2$ (15 mL) was stirred for 24 h at room temperature under N_2 atmosphere. After removal of the excess $SOCl_2$ under vacuum, the residue was washed with anhydrous ethyl ether 5 times and then dried by a N_2 stream. The residue was dissolved in dry MeCN (5 mL), and 4-hydroxybutyl acrylate (1.81 g, 12.4 mmol) was added. Into the reaction mixture in an ice bath, triethylamine (1.26 g, 12.5 mmol) was slowly added. The reaction mixture was stirred for 24 h at room temperature. After water (10 mL) was added, the mixture was extracted 3 times with EA and then the combined organic layer was dried over anhydrous Na_2SO_4. The drying agent was removed by filtration and the solvent was removed in a rotoevaporator. The product was rinsed with ethyl ether 5 times with vigorous stirring and then dried in a N_2 stream. A yellow viscous liquid (6.88 g, 83%) was obtained after drying. DSC (−80 to 60 °C, heating and cooling rate 10 °C/min, N_2): T_g = −70 °C, no other transition found. ^{1}H NMR (400 MHz, CD_3CN, 23 °C): δ 1.31 (m, 2H), 1.58 (m, 2H), 1.72 (m, 4H), 1.85 (m, 2H), 2.29 (t, J = 7, 2H), 3.31 (s, 3H), 3.49 (m, 2H), 3.61 (m, 2H), 3.80 (t, J = 5, 2H), 4.10 (m, 2H), 4.06−4.18 (m, 6H), 4.29 (t, J = 5, 2H), 5.87 (dd, J = 10 (*cis*), J = 2 (gem.), 1H), 6.36 (dd, J = 17 (*trans*), J = 10 (*cis*), 1H), 6.35 (dd, J = 17 (*trans*), J = 2 (gem.), 1H), 7.42 (m, 2H), 8.54 (s, 1H). ^{13}C NMR (100 MHz, acetone-d_6, 23 °C): 25.7, 26.1, 26.7, 29.5, 29.7, 29.8, 29.9, 29.98, 30.00, 30.5, 34.8, 50.5, 50.6, 59.0, 64.4, 64.9, 69.1, 70.9, 72.4, 123.0, 124.0, 129.5, 131.3, 136.8, 166.9, 174.4. HR ESI MS: m/z 481.3307 ([M − Tf_2N]$^+$, calcd. for $C_{26}H_{45}N_2O_6$ 481.3278, error 6.0 ppm).

*1-{ω-[1′-(4′-Acryloyloxy)butoxy]carbonyldecyl}-3-butylimidazolium Tf_2N^- (**3d**)*. A solution of **2d** (6.150 g, 10.4 mmol) in freshly distilled $SOCl_2$ (12 mL) was stirred for 24 h at room temperature under N_2. After removal of the excess $SOCl_2$ under vacuum, the residue was washed with anhydrous ethyl ether 5 times and then dried in a N_2 stream. The residue was dissolved in dry MeCN (20 mL), and 4-hydroxybutyl acrylate (1.656 g, 10.9 mmol) was added. Into the reaction mixture in an ice bath, triethylamine (1.052 g, 10.4 mmol) was slowly added. The reaction mixture was stirred for 24 h at room temperature. After water (20 mL) was added, the mixture was extracted 3 times with EA and then the combined organic layer was dried over anhydrous Na_2SO_4. The drying agent was removed by filtration

Scheme 1. Synthesis of N-diethyleneoxy and N-*n*-butyl Substituted Imidazolium IL Acrylate Monomers 3a, 3b, 3c, and 3d

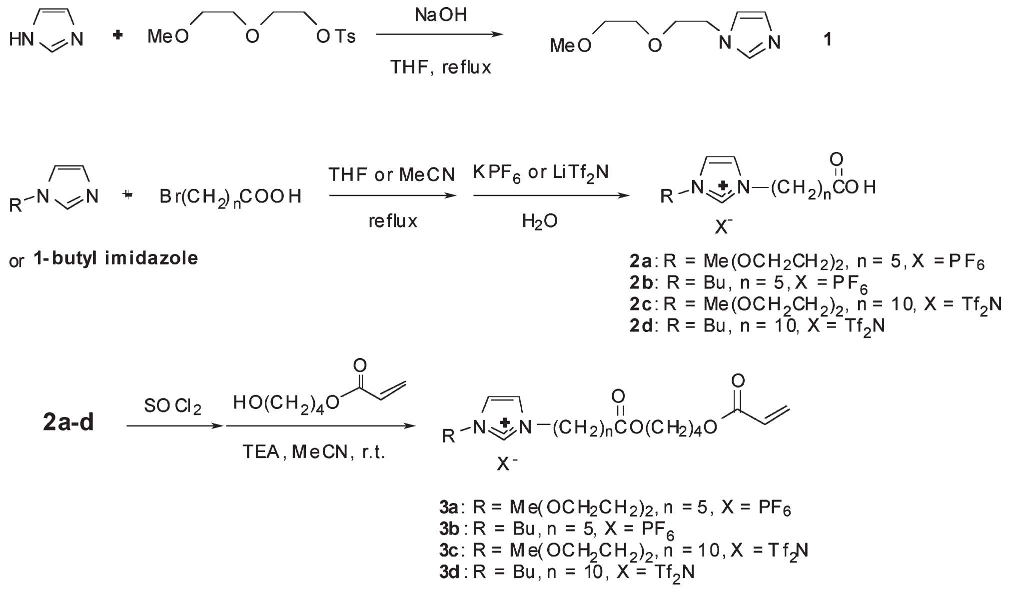

Table 1. DSC and TGA Thermal Analyses of Monomers and Polymers

monomer	T_g (°C, DSC)	polymer	T_g (°C, DSC)	TGA (°C) 5% w/w loss from polymer	ΔT_g (K)
3a	−49	**4a**	−23	326	26
3b	−39	**4b**	−18	334	21
3c	−70	**4c**	−43	318	27
3d	−69	**4d**	−50	382	19

and the solvent was removed on a rotoevaporator. The product was rinsed with ethyl ether 5 times with vigorous stirring. Drying in a vacuum oven at room temperature gave a yellow viscous oil (3.16 g, 42%). DSC (−80 to 60 °C, heating and cooling rate 5 °C/min, N_2): T_g = −69 °C, no other transition found. ^{1}H NMR (400 MHz, CD_3CN, 23 °C): δ 0.94 (t, J = 7, 3H), 1.28 (m, 16H), 1.56 (m, 2H), 1.69 (m, 2H), 1.81 (m, 4H), 2.27 (t, J = 7, 2H), 4.10−4.16 (m, 8H), 5.84 (dd, J = 10 (*cis*), J = 2 (gem.), 1H), 6.13 (dd, J = 17 (*trans*), J = 10 (*cis*), 1H), 6.34 (dd, J = 17 (*trans*), J = 2 (gem.), 1H), 7.38 (ss, 2H), 8.43 (s, 1H). ^{13}C NMR (100 MHz, CD_3CN, 23 °C): δ 13.6, 20.0, 25.7, 26.0, 26.1, 26.7, 29.5, 29.7, 29.9, 29.96, 29.98, 30.4, 32.5, 34.8, 50.3, 50.6, 64.4, 64.9, 123.4, 129.5, 131.3, 136.1, 174.4. HR ESI MS: m/z 435.3246 ($[M - Tf_2N]^+$, calcd. for $C_{25}H_{43}N_2O_4$ 435.3223, error 2.5 ppm).

Radical Polymerizations of Imidazolium Acrylate Monomers. A solution of the imidazolium acrylate monomer and AIBN (2 mol % of the monomer) in degassed MeCN was bubbled with N_2 for 30 min. The solution was stirred for 24 h at 65 °C. After removal of MeCN under vacuum, the residue was stirred with EA. Reprecipitation from acetone into EA was performed 5 times and the precipitated polymer was washed with deionized water twice. Drying in a vacuum oven at 60 °C afforded the highly viscous polymer.

Results and Discussion

Synthesis. The monomers were constructed in three parts: polymerizable acrylate moiety, alkylene spacer connected via an ester linkage, and an N-substituted imidazolium ionic group with hexafluorophosphate (PF_6^-) or bis(trifluoromethanesulfonyl)imide (Tf_2N^-) anions. The imidazolium acrylate monomers were synthesized as shown in Scheme 1. Diethyleneoxy units were introduced to the imidazole ring using tosylated di(ethylene glycol) monomethyl ether under basic conditions in the first step; the end of the ethyleneoxy unit was capped as a methyl ether to avoid hydrogen bonding effects by a hydroxyl group. The quaternization reactions of the 1-substituted imidazoles with 6-bromohexanoic acid and 11-bromoundecanoic acid and ion exchange gave carboxy terminated imidazolium salts **2a** and **2c**, respectively. The quaternization reactions were performed in acetonitrile (MeCN) under reflux for several days. The ion exchange reactions from bromide to PF_6^- or Tf_2N^- were done in aqueous conditions with KPF_6 or $LiTf_2N$. The resulting precipitated salts were washed with deionized water several times and dried in vacuo for 2 days or longer with heat. The absence of bromide residue was confirmed by the Beilstein halide test[32] or treatment with silver nitrate solution. N-*n*-Butyl substituted imidazolium carboxylic acids **2b** (PF_6^- salt) and **2d** (Tf_2N^-) were prepared similarly from 1-butylimidazole. The carboxy imidazolium salts **2a−d** are room temperature ionic liquids (RTILs).

The polymerizable acrylate unit was introduced by esterification of the carboxy imidazolium salts with 4-hydroxybutyl acrylate. After conversion of the caryboxylic acid to the corresponding carbonyl chloride with thionyl chloride, it was reacted with 4-hydroxybutyl acrylate and triethylamine in dry MeCN. The PF_6^- monomers

---

(32) The Beilstein test was done as follows. A copper wire was heated in a burner flame until there was no further coloration of the flame. The wire was allowed to cool slightly, then dipped into the monomer and again heated in the flame. A green flash is indicative of halide ions, whereas pure Tf_2N^- and PF_6^- salts give orange or red colors.

Scheme 2. Polymerization of the Imidazolium Monomers, Effectively Defining the Structure of the Four Imidazolium Polymers 4a, 4b, 4c, and 4d

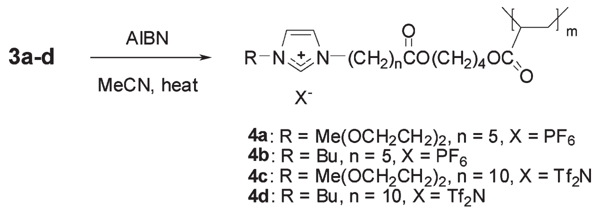

4a: R = $Me(OCH_2CH_2)_2$, n = 5, X = PF_6
4b: R = Bu, n = 5, X = PF_6
4c: R = $Me(OCH_2CH_2)_2$, n = 10, X = Tf_2N
4d: R = Bu, n = 10, X = Tf_2N

(**3a** and **3b**) were purified by several reprecipitations from the good solvent acetone into the poor solvent THF (or ethyl ether), followed by washing with deionized water. The Tf_2N^- monomers (**3c** and **3d**) were purified by extraction with ethyl acetate (EA)/water and washing with ethyl ether to remove unreacted 4-hydroxybutyl acrylate. All the monomers **3a**–**d** are RTILs and they are less viscous than the precursor imidazolium carboxylic acids; they have low T_gs (Table 1 and Scheme 2).

The radical polymerizations of the monomers were performed with 2,2′-azobisisobutyronitrile (AIBN) in degassed MeCN at 65 °C. The product polymers were purified by precipitation with EA, which is a good solvent only for the monomers. The polymers were also washed with deionized water several times to remove water-soluble impurities and dried in vacuo for several days at 60 °C. ^1H NMR spectroscopy confirmed complete conversion into the homopolymers; the vinyl protons of the monomers (δ 5.8, 6.2, and 6.4) disappeared after the polymerizations were completed (Figure 1). The polymers also exhibited some peak broadening. The CH_2 protons that are close to the polymer backbone were broadened, whereas the N-ethyleneoxy or N-butyl protons which are well removed from the polymer backbone still appeared as sharply split signals. Carbon–carbon bond rotation is much faster in the alkyl chains which are far from the polymer backbone and therefore those proton signals remained sharp. Although these polymers generally present difficulties in terms of molecular weight determination, size exclusion chromatography (SEC) using 0.05 M LiBr in DMF in a system calibrated with poly(ethylene oxide) standards afforded M_n = 6.65 kDa and M_w = 15.8 kDa (average of two runs) for **4d**; we believe the other polymers have similar molecular weights and PDIs.

Thermal Analysis. The T_g values of the polymers are 20–30 K higher than those of the corresponding monomers, as reported in Table 1 and shown in Figure 2. The new homopolymers with imidazolium pendant moieties are amorphous; the polymers do not display crystallization or melting in the temperature range of −80 to 200 °C by DSC. Replacing PF_6^- with Tf_2N^- consistently lowered T_g. Monomers have T_g values 21–30 K lower with Tf_2N^-; polymers have T_g values 20–32 K lower with Tf_2N^-. The Tf_2N^- counterion has previously been noted as a plasticizer for imidazolium ionic liquids and their polymers.[18] A significant anion effect on thermal stability occurs only in the polymers with an N-butyl substituent; TGA 5% weight loss of **4d** (Tf_2N^-) takes place at 382 °C, but takes place at 334 °C in **4b** (PF_6^-). The N-diethyleneoxy polymers do not show much difference; the TGA 5% weight loss of **4a** (PF_6^-) is 326 °C and that of **4c** (Tf_2N^-) is 318 °C. The lower thermal stability of the ethyleneoxy polymers vs the butyl polymers is due to the presence of the more labile C–O–C bonds.

Ionic Conductivity Measured by Dielectric Spectroscopy. As expected, ionic conductivities are lower for the polymers than the monomers (Tables 2 and 3). The decreased ionic conductivity in the polymers can be mostly explained by the decrease in the segmental motion

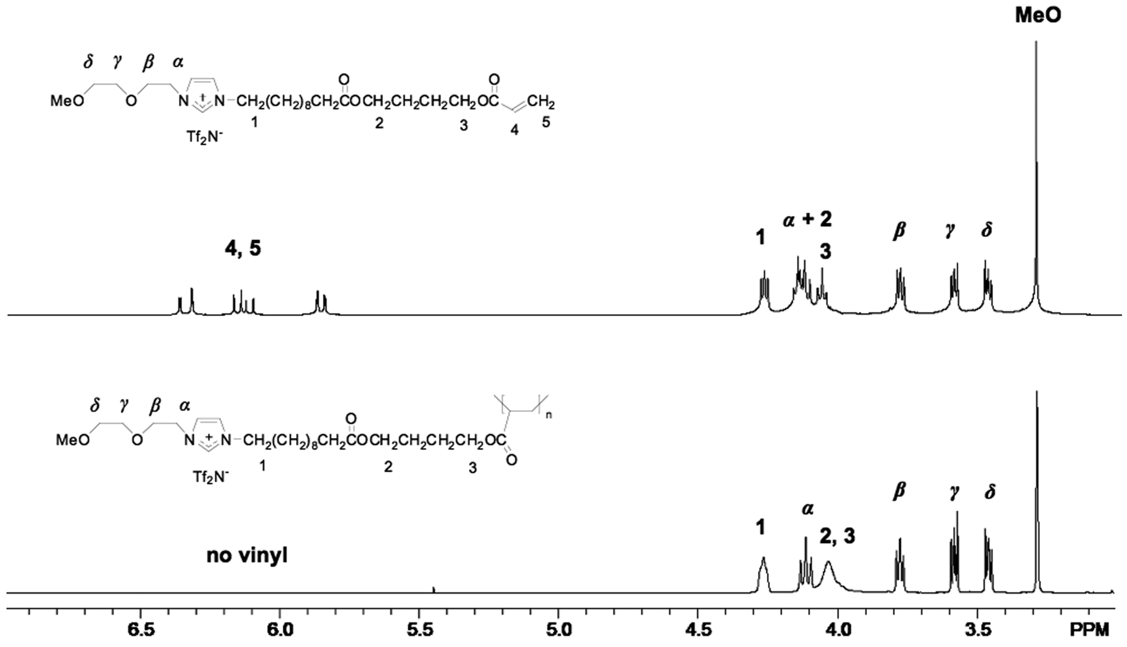

Figure 1. Partial 400 MHz ^1H NMR spectra of monomer **3c** (upper) and polymer **4c** (lower) in CD_3CN at 23 °C. After polymerization, the vinyl proton peaks (4 and 5 in the upper spectrum) disappear and protons 1, 2, 3 are broadened. However, the ethyleneoxy peaks (α, β, γ, δ) are still sharply split in the polymer spectrum (lower), as they are in the monomer spectrum (upper).

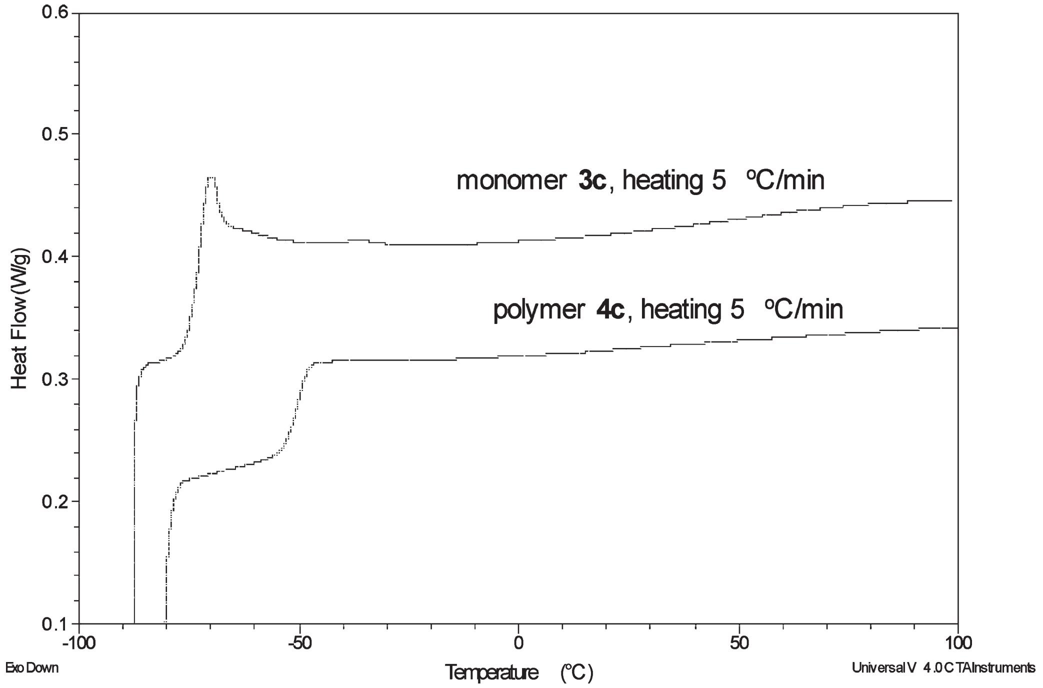

Figure 2. DSC thermograms of monomer **3c** and polymer **4c**, showing the increase in T_g on polymerization.

Table 2. Ionic Conductivities of PF_6^- Monomers and Polymers

compound	25 °C conductivity (Scm^{-1})
3a	3.5×10^{-5}
3b	1.3×10^{-5}
4a	1.8×10^{-6}
4b	3.9×10^{-7}

Table 3. Ionic Conductivities of Tf_2N^- Monomers and Polymers

compound	25 °C conductivity (Scm^{-1})
3c	2.2×10^{-4}
3d	1.2×10^{-4}
4c	2.8×10^{-5}
4d	1.8×10^{-5}

in the polymer relative to the monomer reflected in a change in T_g.[13] There is also a significant effect from the diethyleneoxy vs the butyl terminal N-substituents on ionic conductivity for PF_6^- monomers and polymers. The room temperature ionic conductivity of the N-diethyleneoxy monomer **3a** (3.5×10^{-5} Scm^{-1}) is slightly higher than that of N-butyl substituted monomer **3b** (1.3×10^{-5} Scm^{-1}). After polymerization, the conductivity of the ethyleneoxy substituted polymer **4a** (1.8×10^{-6} Scm^{-1}) is almost 5-fold higher than that of the butyl substituted polymer **4b** (3.9×10^{-7} Scm^{-1}). For the Tf_2N^- polymers, the room temperature ionic conductivity of ethyleneoxy substituted **4c** (2.8×10^{-5} Scm^{-1}) is 50% higher than that of butyl substituted polymer **4d** (1.8×10^{-5} Scm^{-1}). The diethyleneoxy units on the imidazolium cation afford a higher ionic conductivity at low temperature, but a negligible effect at high temperature, relative to the butyl substituted system as shown in Figure 3. Ohno observed with brush imidazolium Tf_2N^- polymers that dodecyl spacers possessed slightly higher ionic conductivity than the ethyleneoxy [$(CH_2CH_2O)_8$] containing polymer.[14] The spacers of his polymers were placed between the polymer backbone and the imidazolium unit. However, in our polymer the diethyleneoxy substituent, which is placed far from the polymer backbone, plays a more important role in the ion conduction below room temperature. These terminal ethyleneoxy moieties may have interactions with other imidazolium rings[33] and these interactions are more significant below room temperature.

Electrode Polarization Analysis. To better understand the conduction mechanism, it is necessary to distinguish whether the increase in ionic conductivity is due to a larger fraction of conducting ions or to an increase in ion mobility, because ionic conductivity is the product of charge e, number density of conducting ions p, and their mobility μ.

$$\sigma_{DC} = ep\mu \tag{1}$$

A physical model of electrode polarization (EP) makes it possible to separate ionic conductivity into the contributions of conducting ion concentration and ion mobility[24-27] as has recently been done for other single-ion conductors above T_g.[28-30] Electrode polarization occurs at low frequencies, where the transporting ions have sufficient time to polarize at the blocking electrodes during the cycle. That polarization manifests itself in (1) an increase in the effective capacitance of the cell (increasing the dielectric constant) and (2) a decrease in the in-phase part of the conductivity, as the polarizing ions reduce the field experienced by the transporting ions. The natural time scale for conduction is the time at which counterion motion becomes diffusive

$$\tau_\sigma \equiv \frac{\varepsilon_s \varepsilon_0}{\sigma_{DC}} \tag{2}$$

---

(33) Smith, G. D.; Borodin, O.; Li, L.; Kim, H.; Liu, Q.; Bara, J. E.; Gin, D. L.; Noble, R. D. *Phys. Chem. Chem. Phys.* **2008**, *10*, 6301.

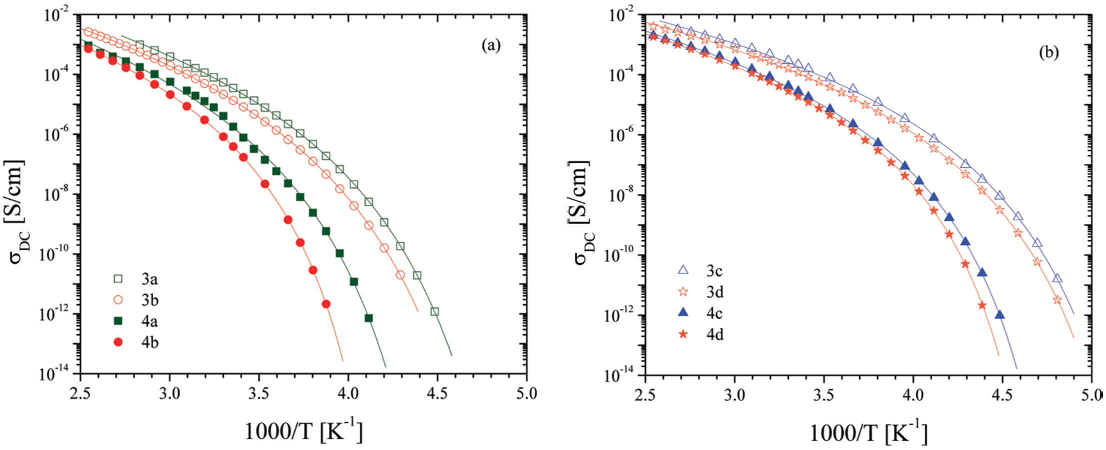

Figure 3. Temperature dependence of ionic conductivities of (a) PF_6^- monomers and polymers and (b) Tf_2N^- monomers and polymers. Monomers (open symbols) have consistently higher conductivities than their polymers (filled symbols). Lines indicate fits to eq 9.

in which ε_s is the static relative permittivity of the sample, ε_0 is the permittivity of vacuum, and σ_{DC} is the d.c. conductivity, evaluated from a roughly 3-decade frequency range over which the in-phase part of the conductivity $\sigma'(\omega) = \varepsilon''(\omega)\varepsilon_0\omega$ is independent of frequency. At low frequencies the conducting ions start to polarize at the electrodes and fully polarize at the electrode polarization time scale

$$\tau_{EP} \equiv \frac{\varepsilon_{EP}\varepsilon_0}{\sigma_{DC}} \tag{3}$$

in which ε_{EP} is the (considerably larger) effective permittivity after the electrode polarization is complete. The Macdonald/Coelho model[24-28] treats electrode polarization as a simple Debye relaxation with loss tangent.

$$\tan\delta = \frac{\omega\tau_{EP}}{1+\omega^2\tau_\sigma\tau_{EP}} \tag{4}$$

In practice, the loss tangent associated with electrode polarization is fit to eq 4 to determine the electrode polarization time τ_{EP} and the conductivity time τ_σ. The Macdonald/Coelho model then determines the number density of conducting ions p and their mobility μ from τ_{EP}

$$p = \frac{1}{\pi l_B L^2}\left(\frac{\tau_{EP}}{\tau_\sigma}\right)^2 \tag{5}$$

$$\mu = \frac{eL^2\tau_\sigma}{4\tau_{EP}^2 kT} \tag{6}$$

in which $l_B \equiv e^2/(4\pi\varepsilon_s\varepsilon_0 kT)$ is the Bjerrum length, L is the spacing between electrodes, e is the elementary charge, k is the Boltzmann constant, and T is absolute temperature.

Conducting Ion Content. The temperature dependence of the number density of conducting ions p calculated from eq 5 is plotted as shown in Figure 4 for the polymerizable ionic liquid acrylate monomers (open symbols) and their polymers (filled symbols), and the fraction of ions participating in conduction (p/p_0: p_0 is the total anion number density) is shown in the Figure 4 inset. The temperature dependence of conducting ion concentration for these monomers and polymers is well described by an Arrhenius equation

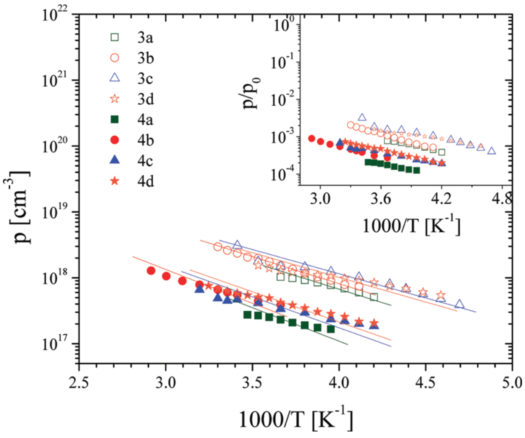

Figure 4. Temperature dependence of conducting ion number density p. The inset shows the fraction of counterions in the conducting state (p divided by the total anion concentration p_0). Monomers (open symbols) have consistently higher conducting ion contents than their polymers (filled symbols). Lines are fits to eq 7 with the activation energy as the sole fitting parameter (listed in Table 4).

$$p = p_0 \exp\left(-\frac{E_a}{RT}\right) \tag{7}$$

in which p_0 is the total anion concentration (all anions are in conducting states at all times as $T \rightarrow \infty$) here estimated from density determined by the group contribution method[34] and E_a is an activation energy for conducting ions. The activation energy of the conducting ions in these materials is an effective experimental measure of the binding energy of an ion pair (the electrostatic attraction between cation and anion, mediated by the environment). The activation energies determined by fitting the data in Figure 4 to eq 7 are listed in Table 4. The inset in Figure 4 indicates that the fraction of ions in a conducting state at any instant in time is quite low, ~0.1% at or near room temperature. This is similar to observations on other

---

(34) Van Krevelen, D. W.; Hoftyzer, P. J. *Properties of Polymers: Their Estimation and Correlation with Chemical Structure*; Elsevier: New York, 1976.

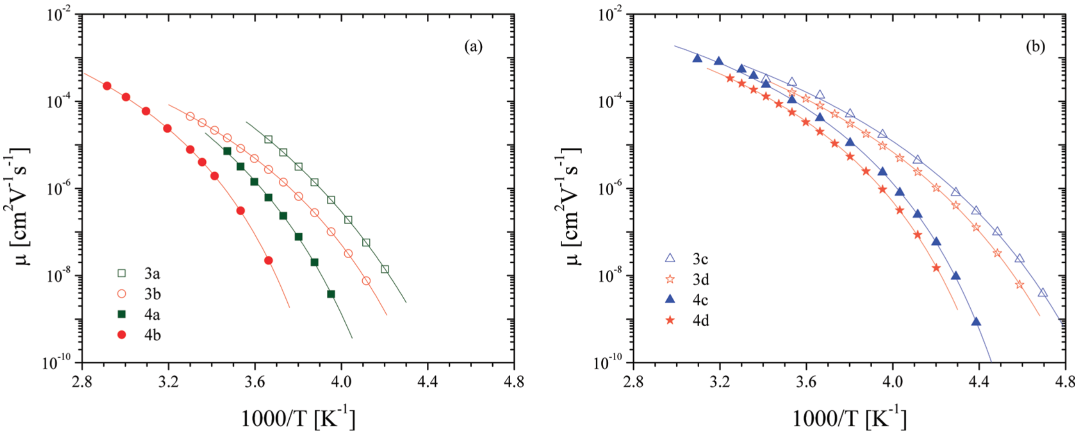

Figure 5. Temperature dependence of conducting ion mobilities for (a) PF_6^- monomers and polymers and (b) Tf_2N^- monomers and polymers. Monomers (open symbols) have consistently higher mobilities than their polymers (filled symbols). Lines are fits to eq 8 with fitting parameters listed in Table 4.

Table 4. Parameters of the VFT Equation for Conducting Ion Mobility, eq 8, and the Arrhenius Equation for Conducting Ion Concentration, eq 7

compound	conducting ion mobility				conducting ion concentration	
	$\log \mu_\infty$ (cm^{2}V^{-1}s^{-1})	D_μ	T_0 (K)	$T_g - T_0$ (K)	$\log p_0$ (cm^{-3})	E_a (kJ/mol)
3a	0.8	3.3	172	52	21.1	15.5
3b	−0.9	2.1	188	46	21.2	15.7
3c	−0.3	2.4	164	39	21.0	14.1
3d	−0.3	2.4	167	37	21.0	14.3
4a	−0.1	2.3	197	53	21.1	19.4
4b	−0.6	1.7	221	34	21.2	19.6
4c	−0.5	1.7	191	39	21.0	18.0
4d	−0.7	1.7	193	30	21.0	17.6

single-ion conducting ionomers with sulfonate ions bound to the chain and alkali metal counterions.[28−30] Interestingly, the monomers (**3a**, **3b**, **3c**, and **3d**) have somewhat higher conducting ion concentrations than the polymers (**4a**, **4b**, **4c**, and **4d**). Part of the reason for that is the monomers are similar to conventional ionic liquids, with both cations and anions participating in conduction, whereas for the polymers only the anions are mobile. The activation energy is $E_a = 15.6$ kJ/mol for both PF_6^- monomers (**3a** and **3b**) and $E_a = 14.2$ kJ/mol for both Tf_2N^- monomers (**3c** and **3d**). Both of these activation energies increase by about 25% on polymerization, as the PF_6^- polymers (**4a** and **4b**) have $E_a = 19.5$ kJ/mol and the Tf_2N^- polymers (**4c** and **4d**) have $E_a = 17.8$ kJ/mol. The lower activation energy in Tf_2N^- monomers and polymers indicates a lower binding energy of the larger Tf_2N^- ions to the imidazolium ions compared to the PF_6^- ions.[11]

Mobility of the Conducting Ions. The ionic mobility determined from the EP model is displayed in Figure 5 vs inverse temperature. We fit these data to the Vogel−Fulcher−Tammann (VFT) equation

$$\mu = \mu_\infty \exp\left(-\frac{D_\mu T_0}{T - T_0}\right) \qquad (8)$$

in which μ_∞ is the ion mobility as $T \to \infty$, D_μ is the so-called strength parameter related to the divergence from Arrhenius temperature dependence, and T_0 is the Vogel temperature at which the free volume extrapolates to zero. The fit parameters μ_∞, D_μ, and T_0 are given in Table 4. The VFT dependence of ion mobility reflects the coupling of segmental motion of polymer backbone and ion motion. Like ionic conductivity, the ionic mobility of the N-diethyleneoxy substituted monomers (**3a** and **3c**) and polymers (**4a** and **4c**) is higher than that of the N-butyl substituted monomers (**3b** and **3d**) and polymers (**4b** and **4d**) (Figure 5). Watanabe and co-workers[35,36] showed that the conductivity/diffusion of ionic liquids deviates from the Nernst−Einstein approximation, indicating that the effective number of ions available for conduction is reduced through formation of ion pairs having a zero net charge, that still contribute to diffusion. Hence, it is a reasonable assumption that under the influence of electrostatic interactions counterions interacting with ion pairs might form triple ions which contribute to the conductivity. The fact that the imidazolium cations are attached to the polymer chain suggests that the PF_6^- and Tf_2N^- anions, assisted by the activated motion of the polymer host, could exchange themselves between one ion pair and a neighboring one. In other words, the mobility will depend not only on the segmental motion but also an energy barrier for anion hopping. The enhanced ion mobility in the N-diethyleneoxy substituted monomers and polymers, therefore, may be interpreted as simply lowering this barrier. The ether-functionalized imidazolium cations have an energetic preference for the gauche conformation that allows interactions between the ether oxygen atoms and the hydrogen atoms

---

(35) Tokuda, H.; Hayamizu, K.; Ishii, K.; Susan, M. A. B. H.; Watanabe, M. *J. Phys. Chem. B* **2004**, *108*, 16593.

(36) Tokuda, H.; Ishii, K.; Susan, M. A. B. H.; Tsuzuki, S.; Hayamizu, K.; Watanabe, M. *J. Phys. Chem. B* **2006**, *110*, 2833.

Table 5. Fitting Parameters for the Temperature Dependence of d.c. Ionic Conductivity Using eq 9

compound	ionic conductivity				
	$\log(ep_{\infty}\mu_{\infty})$(S/cm)	E_a (kJ/mol)	D_{σ}	T_0 (K)	$T_g - T_0$ (K)
3a	1.6	15.5	2.0	185	39
3b	1.5	15.7	2.1	187	47
3c	1.0	14.1	1.6	174	29
3d	0.9	14.3	1.6	175	29
4a	1.6	19.4	1.9	203	47
4b	1.4	19.6	1.6	221	34
4c	1.1	18.0	1.3	194	36
4d	0.9	17.6	1.3	198	25

of the imidazolium ring.[33,37] The H$-$O$_{\text{ether}}$ interactions also result in a reduction of cation$-$anion pair dissociation energy (effectively stabilizing the cation separated from its anion) which results in a lower energy barrier for anion hopping. This more rapid dynamics of ionic liquids with ether groups is also observed in viscosity[38,39] and ion-diffusion coefficients.[40] On the other hand, the difference in ionic mobility between the N-diethyleneoxy and the N-butyl substituted Tf_2N^- polymers is smaller than that of PF_6^- polymers. This is likely caused by the Tf_2N^- counterions being better plasticizers (lowering T_g) than the considerably smaller PF_6^- counterions.

On the basis of both ion mobility and conducting ion concentration, we can determine the temperature dependence of ionic conductivity by combining eq 1 with eqs 7 and 8

$$\sigma = ep\mu = ep_{\infty}\mu_{\infty}\exp\left(-\frac{D_{\sigma}T_0}{T - T_0}\right)\exp\left(-\frac{E_a}{RT}\right) \tag{9}$$

E_a was fixed to the activation energy determined by fitting conducting ion content to eq 7. As a result, we observe that a value of T_0 obtained using eq 9 in Table 5 is slightly higher than using eq 8 in Table 4. Conductivity is measured over a considerably wider temperature range than mobility, since EP can only be analyzed over a smaller T-range, and in particular, since conductivity is always measured closer to T_g than mobility, the D_{σ} and T_0 values from fitting conductivity data to eq 9, listed in Table 5, are more reliable. This result also points out that larger $T_g - T_0$ always is associated with larger D_{σ} and that both suggest lower fragility.

Conclusion

Four new polymerizable ionic liquid imidazolium acrylate monomers and their corresponding polymers, which contain either an N-*n*-butyl or an N-diethyleneoxy substituent on the imidazolium unit and either PF_6^- of Tf_2N^- counterions, have been synthesized and their properties have been characterized. The introduction of diethyleneoxy vs *n*-butyl units on the imidazolium cation affected the thermal and electrical properties of the polymers. The effect is clearly shown in room temperature conductivity; the ionic conductivity of diethyleneoxy substituted **4a** is 5 times higher than that of the butyl polymer **4b**; likewise that of diethyleneoxy substituted **4c** is 50% higher than that of the butyl polymer **4d**.

A physical model of EP makes it possible for ionic conductivity to be separated into (1) conducting ion number density and (2) conducting ion mobility. The reduction in cation$-$anion interactions due to the ether tail leads to the higher mobility of the diethyleneoxy substituted imidazolium monomers and polymers, and increased conductivity. Beyond the conductivity time scale τ_{σ} counterion motion becomes diffusive, with all counterions contributing equally to ion conduction. Even though electrode polarization occurs on a much longer time scale, the conducting ion content evaluated from the EP model is the number density of ions in a conducting state in any snapshot, which sets the boundary condition for the solution of the Poisson$-$Boltzmann equation. For this reason, only a small fraction of total ions exist as conducting ions at any given instant in time in these materials and in other ionomers.

Acknowledgment. We are very appreciative of financial support from the U.S. Army Research Office under grant W911NF-07-1-0452 Ionic Liquids in Electro-Active Devices (ILEAD) MURI. We are also grateful to Prof. James McGrath and Tim Long (VPI&SU) for use of their thermal analysis equipment, Prof. James Runt (Penn State) for use of his dielectric spectrometer, and Prof. Qiming Zhang (Penn State) for discussions. We are also grateful to Prof. Yossef A. Elabd and Mr. Yuesheng Ye of Drexel University for the SEC measurement on **4d**.

Supporting Information Available: ^{1}H NMR spectra of new compounds **2a**, **2b**, **2c**, **2d**, **3a**, **3b**, **3c**, **3d**; SEC trace for polymer **4d**; frequency dependence of the loss tangent for **3a**, **4a**, **3b**, **4b**, **3c**, **4c**, **3d**, **4d**. This material is available free of charge via the Internet at http://pubs.acs.org.

---

(37) Fei, Z.; Ang, W. H.; Zhao, D.; Scopelliti, R.; Zvereva, E. E.; Katsyuba, S. A.; Dyson, P. J. *J. Phys. Chem. B* **2007**, *111*, 10095.

(38) Branco, L. C.; Rosa, J. N.; Ramos, J. J. M.; Afonso, C. A. M. *Chem. Eur. J.* **2002**, *8*, 3671.

(39) Zhou, Z. B.; Matsumoto, H.; Tatsumi, K. *Chem. Eur. J.* **2006**, *12*, 2196.

(40) Smith, G. D.; Borodin, O.; Li, L.; Kim, H.; Liu, Q.; Bara, J. E.; Gin, D. L.; Nobel, R. *Phys. Chem. Chem. Phys.* **2008**, *10*, 6301.